Available online at www.sciencedirect.com
SCIENCE DIRECT®
Chemical Physics Letters 407 (2005) 477–481
CHEMICAL PHYSICS LETTERS
www.elsevier.com/locate/cplett

Blue upconversion emission of Tm^{3+}–Yb^{3+} in ZrO_2 nanocrystals: Role of Yb^{3+} ions

Amitava Patra [a,*], Sujata Saha [a], Márcio A.R.C. Alencar [b], Nikifor Rakov [b], Glauco S. Maciel [b]

[a] *Sol-Gel Division, Central Glass & Ceramic Research Institute, Jadavpur, Kolkata 700 032, India*
[b] *Departamento de Física, Universidade Federal de Pernambuco, 50670-901 Recife, PE, Brazil*

Received 2 March 2005; in final form 31 March 2005
Available online 20 April 2005

Abstract

The effect of Yb^{3+} ions on the blue upconversion (UPC) emission of Yb^{3+}–Tm^{3+} co-doped ZrO_2 nanocrystals is reported. The blue (490 nm) UPC emission is due to $^1G_4$–$^3H_6$ transition of Tm^{3+} and the pump power dependence of this UPC emission band are cubic indicating that three excitation photons are involved in the UPC process. An additional UPC emission band at 505 nm is observed when the Yb^{3+} concentration is above 1.25 mol%. The pump power dependence of the emission at 505 nm is quadratic, indicating that this emission may have its origin from excited Yb^{3+} pairs producing cooperative UPC.

1. Introduction

There has been a growing interest in the study of rare-earth (RE) doped materials for frequency upconversion (UPC) of infrared radiation into shorter wavelengths for photonic and biophotonic applications [1–11]. Intensive research efforts are therefore devoted to design and tune of the upconversion properties of these materials. A very broad range of unprecedented optical properties can be observed by changing the host lattice and dopant concentration. From the fundamental point of view, the physical understanding of UPC emission of rare-earth ions in oxide nanocrystals and the way it changes with size, crystal phase and concentration is not well understood. It is well known that the electronic f–f transitions of rare-earth ions involve electrons which are localized in atomic orbitals of the ions. Therefore, no size-dependent quantization effect (due to confinement of delocalized electrons) is expected in these transitions. However, nanoscopic interactions play key roles in controlling the excitation dynamics. Recently, we have reported the influences of dopant concentration, crystal size and crystal structure on the emission properties of erbium ions in oxide nanocrystals [8–12]. Among the oxide hosts, the zirconia matrix seems to be an ideal medium for preparation of highly luminescent materials because it is chemically and photochemically stable, has a high refractive index and low phonon energy [8]. Studies of the upconversion process in thulium (Tm^{3+}) doped materials are of great interest because Tm^{3+} exhibits strong fluorescence in the violet and blue region [6]. The main goal of this work is to study the upconversion luminescence of Tm^{3+}:Yb^{3+} co-doped ZrO_2 matrix and how this property changes with changing co-dopant concentration of Yb^{3+}-ions. Apparently, there is no report on the study of blue UPC emission of Tm^{3+}:Yb^{3+} co-doped ZrO_2 nanocrystals.

This report includes the synthesis and investigations of how the concentration of Yb^{3+} ions affects the

* Corresponding author. Fax: +91 33 24730957.
E-mail address: apatra@cgcri.res.in (A. Patra).

0009-2614/$ - see front matter © 2005 Elsevier B.V. All rights reserved.
doi:10.1016/j.cplett.2005.03.135

upconversion emission properties of Yb^{3+} and Tm^{3+} co-doped ZrO_2 nanocrystals prepared via a sol-emulsion-gel process.

2. Experimental procedure

The sol-emulsion-gel [8–12] method was used for the preparation of Yb^{3+}–Tm^{3+} co-doped ZrO_2 nanoparticles. No report has been found on the preparation of sol-emulsion-gel synthesis of Yb^{3+}–Tm^{3+} co-doped ZrO_2 nanoparticles, to our knowledge. Zirconia propoxide (Fluka), thulium acetate (Aldrich) and ytterbium acetate (Aldrich) were used as the starting materials. First, three milliliters of glacial acetic acid was slowly added to 10 ml of zirconia propoxide and stirred for 30 min. Then 20 ml of *n*-propanol was added to the solution, which was further stirred for 15 min at room temperature. Four milliliters of 50% aqueous acetic acid was slowly added to the above solution under stirring which resulted in a clear transparent solution. Then, required amount of ytterbium and thulium acetate was added to this solution. The emulsified sol droplets were obtained through water-in-oil (w/o) type emulsions with cyclohexane and sorbitan monooleate (Span 80, fluka) as the organic liquid (oil phase) and non-ionic surfactant, respectively. The support solvent containing 5 vol% of span 80 in cyclohexane was used for emulsification, i.e., for the preparation of water-in-oil (w/o) type emulsion in the present study. The volume ratio of the sol and cyclohexane was 1:4. A measured amount of ytterbium and thulium acetate doped zirconia sol was then dispersed in the solvent under stirring condition. The sol droplets formed in the process were then gelled by the controlled addition of a base. The gel particles were separated by centrifugation followed by washing with acetone and methanol. The product was dried at 60 °C in air for 12 h. The dried materials were ground and calcined at 1000 and 1150 °C for 1 h.

The crystalline phases of sintered powders were identified by X-ray diffraction (XRD). The spectra were recorded from 20° to 70° with increments of 0.5°. The crystallite sizes of the nanocrystals were calculated following the Scherrer's equation:

$$D = K\lambda/\beta\cos\Theta, \quad (1)$$

where $K = 0.9$, D represents crystallite size (Å), λ, the wavelength of Cu Kα radiation and β the corrected half-width of the diffraction peak. We pressed the particles to form a smooth, opaque flat disk for optical study. The samples were irradiated with a diode laser emitting at 980 nm and the UPC fluorescence (easily visible) was collected with a multimode fiber connected to a monochromator attached to a photomultiplier tube. The sample luminescence dynamics were analyzed using a digital fast oscilloscope (100 MHz). The UPC signal was sent to a personal computer for processing. The measurements were performed at room temperature.

3. Results and discussion

The powder XRD patterns (Fig. 1) show the presence of monoclinic, tetragonal and cubic phases of different compositions of Yb^{3+}–Tm^{3+} co-doped ZrO_2 nanocrystals obtained after annealing at different temperatures. Two strongest lines are at 28.2° $(1,1,-1)$ and 31.4° $(1,1,1)$ for the monoclinic phase (m) (JCPDS 37 1484) and the strongest line at 30.17° (1 1 1) is for the metastable tetragonal phase (JCPDS 17 0923). The spectra show that the dominant structure is the monoclinic phase (m) for 1000 °C annealed Yb^{3+}–Tm^{3+} (1.25:0.25 mol%) co-doped ZrO_2 nanocrystals and the percentage of monoclinic phase is 65.97%. However, the tetragonal phase (t) is dominant for 1000 °C annealed Yb^{3+}–Tm^{3+} (2.5:0.25 mol%) co-doped ZrO_2 nanocrystals. It is interesting to note that the percentage of tetragonal phase formation increases (75.87–84.10%) with increasing the annealing temperature from 1000 to 1150 °C for Yb^{3+}–Tm^{3+} (2.5:0.25 mol%) co-doped ZrO_2 nanocrystals. In case of 1000 °C annealed Yb^{3+}–Tm^{3+} (5:0.25 mol%) co-doped ZrO_2 nanocrystals, only cubic phase (c) (JCPDS 27 0997) is obtained. The diameter of rare-earth ion (M^{3+}) is larger than that of Zr^{4+}; the introduction of such ion will induce the change of ZrO_2 lattice. At low dopant concentrations, monoclinic structure of zirconia is observed with space group of $P2_1/c$, where each Zr atom is in sevenfold coordination with oxygens. It is seen that tetragonal phase increases with increase the temperature (1000–1150 °C) and concentration of

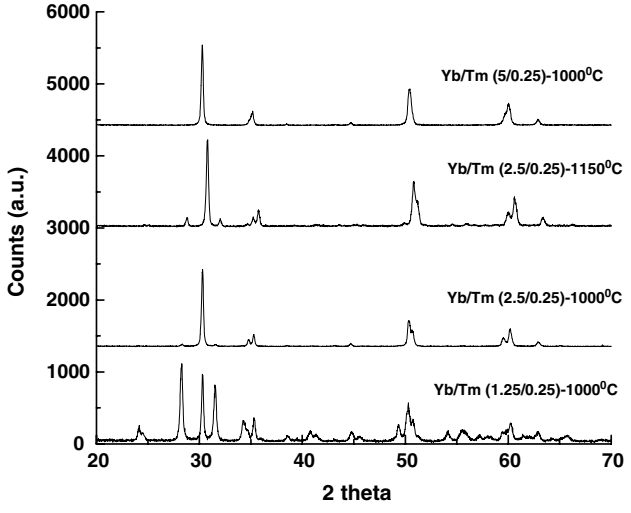

Fig. 1. Powder X-ray diffraction patterns of different compositions of Yb^{3+} and Tm^{3+} co-doped ZrO_2 nanocrystals obtained after annealing at 1000 and 1150 °C.

Yb^{3+}-ions from 1.25 to 2.5 mol%. The crystal structure of tetragonal ZrO_2 is a body centered lattice with the space group $P4_2/nmc$. The effect of increasing the tetragonal phase is due to removal of oxygen vacancies, which helps to reduce the nonradiative relaxation. It is well known that the stabilization of the fluorite-type zirconia lattice can be achieved by oxygen vacancies mechanism for trivalent dopants [13]. For ZrO_2–3.0 mol% Yb_2O_3, Michel et al. [14] proposed tetragonal zirconia as a layer structure in which tetragonality is attributed to the strong bonding of $Zr–O_I$ within the layers and weak bonding of $Zr–O_{II}$ between layers. However, at higher concentration (5.0 mol% Yb), the cubic phase (space group $Fm3m$) becomes dominant with larger amounts of O^{2-} ion vacancies, which influence the nonradiative relaxation. These results clearly indicate the crystal structure and crystal symmetry are depending on the annealing temperature and concentration of dopant ions. The average crystal sizes (using Eq. (1)) are 31 ± 2 and 36 ± 2 nm (calculated from tetragonal phase) for 1000 and 1150 °C for Yb^{3+}–Tm^{3+} (2.5:0.25) co-doped ZrO_2 nanocrystals, respectively. Therefore, with increasing the temperature of annealing the crystal size increases due to growth of particles. This dependence indicates the important role on the Yb^{3+} dopant content as a control for the crystal phase and crystal size. This results show how the crystal phase and crystal size can be controlled by changing the Yb^{3+} concentration and annealing temperature. The SEM observation of Yb^{3+}–Tm^{3+} (2.5:0.25) co-doped ZrO_2 nanocrystals prepared at 1150 °C shows that the particles are in aggregated form and the average diameter is about 70–80 nm.

The upconverted luminescence of different compositions of Yb^{3+}–Tm^{3+} co-doped ZrO_2 nanocrystals prepared at different temperature of annealing are shown in Fig. 2. The UPC emissions bands centered at 476 and 490 nm are observed in all studied samples under excitation at 980 nm. Generally, the f–f transition is very narrow and exhibit multiple structures derived from electronic interactions, as well as spin–orbit coupling. The emission band at 476 nm arises due to the effect of crystal field. It is also seen that the intensities of these bands increase with increasing the concentration of Yb^{3+} and further decrease when the concentration of Yb^{3+} ions reaches at 5.0 mol%, which may be due to concentration quenching [12]. A significant observation is made when the concentration of Yb^{3+} ions is higher than 1.25 mol% in Yb^{3+}–Tm^{3+} co-doped ZrO_2 nanocrystals. That is a new emission band at 505 nm. Here, we can definitely say, concentration of Yb^{3+} ions has also played an important role in the generation of new upconversion emission band. To explain the mechanisms responsible for the UPC processes observed in our samples, we use the energy level diagram as shown in Fig. 3. First, excitation photons of 980 nm are strongly absorbed by isolated Yb^{3+} ions because the diode laser wavelength matches with the absorption transition between the ground state ($^2F_{7/2}$) and the excited level ($^2F_{5/2}$) of Yb^{3+}. These ions act as sensitizers and this absorption process is strongly dependent on the distance between neighboring ions. After absorption of photons by Yb^{3+}, energy transfer takes place between Yb^{3+} and Tm^{3+}. The first step of this energy transfer process occurs from excited state $^2F_{5/2}$ of Yb^{3+} to level $^3H_5$ of Tm^{3+}. Then, the population

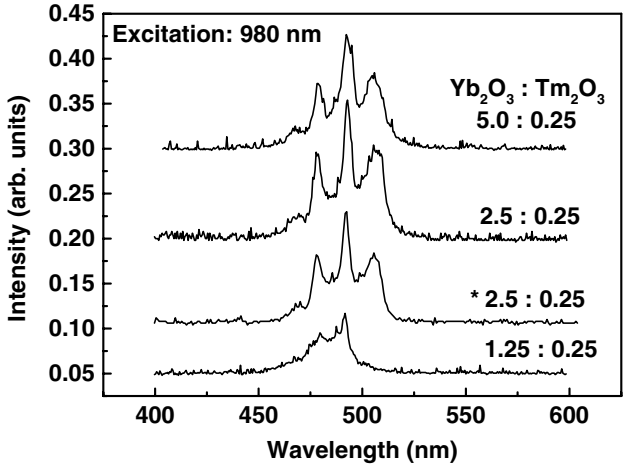

Fig. 2. Upconverted emission spectra of different compositions of Yb^{3+} and Tm^{3+} co-doped ZrO_2 nanocrystals obtained after annealing at 1000 and 1150 °C (shown with the symbol '*').

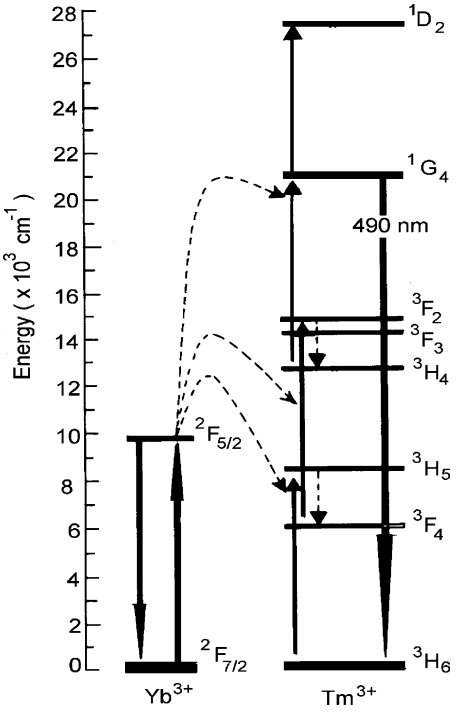

Fig. 3. The energy level diagram for Yb^{3+} and Tm^{3+} ions under 980 nm excitation.

accumulated at level $^3H_5$ decays rapidly to the metastable level $^3F_4$ of Tm^{3+}. The second step of energy transfer takes place from another excited Yb^{3+} (at level $^2F_{5/2}$) to Tm^{3+} populating levels $^3F_2$ and $^3F_3$ from level $^3F_4$. Then the population decays to level $^3H_4$. The next step of ET occurs from a third excited Yb^{3+} (at level $^2F_{5/2}$) to Tm^{3+} populating the high-lying excited state $^1G_4$ from level $^3H_4$. The bright blue peaked at 476 and 490 nm are assigned to $^1G_4$–$^3H_6$ transition of Tm^{3+} and it is a three-step energy transfer (ET) process from Yb^{3+} ions. The emission line peaked at ~505 nm does not appear in the spectrum of the sample with lower doping concentration of Yb^{3+} and therefore this emission are not originated from Tm^{3+} ions. In 0.25 mol%, Tm concentration, the mean distance (R) between the Tm^{3+} ions is estimated by $R = 0.62/(N)^{1/3}$ (where N is the concentration of ions) to be 1.81 nm, but the distance between the Yb^{3+} ions in Yb^{3+}–Tm^{3+} co-doped ZrO_2 nanocrystals are 1.06, 0.84 and 0.66 nm for 1.25, 2.5 and 5.0 mol% Yb^{3+} ions concentration, respectively [15]. It is known that the ions in low concentration are usually randomly distributed in the host lattice and the distances are too far apart but at higher concentration, the distances between two ions are shortened, thus leading to formation of pairs. Therefore, we believe that the emission at 505 nm may be cooperative UPC from Yb^{3+} pairs [16]. The mechanism responsible for this UPC process is shown in Fig. 4. First, the excitation photons at 980 nm are strongly absorbed by isolated Yb^{3+} ions and then by dipole–dipole interaction with neighboring Yb^{3+} ions due to high concentration give rise to the Yb^{3+}–Yb^{3+} pair formation which gives the emission at 505 nm. In order to analyze the UPC mechanism which populates the $^1G_4$ level, the pump power dependence of the emission from $^1G_4 \rightarrow {}^3H_6$ level at 490 nm was investigated on excitation intensity at 980 nm and the results are shown in Fig. 5 (squares). The experimental data have been fit with a straight line with slope of ~3 which indicates that the blue UPC emission from Tm^{3+} is a three photon process. However, the pump power dependence of the emission at 505 nm was investigated on

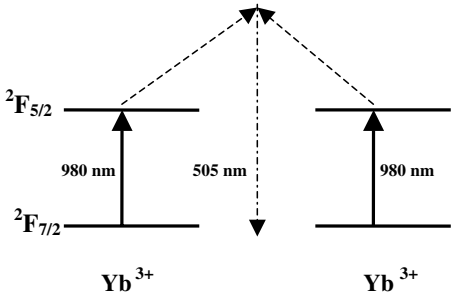

Fig. 4. Energy level diagram of Yb^{3+}–Yb^{3+} pairs and proposed cooperative energy transfer pathways is shown as dotted lines and the upconversion emission as dashed lines.

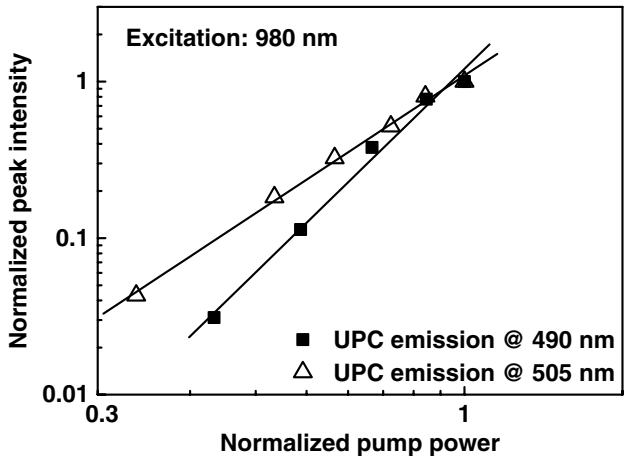

Fig. 5. Variation of the upconverted emission intensities with pump power for Yb^{3+} (2.5 mol%)–Tm^{3+} (0.25 mol%) co-doped ZrO_2 nanocrystals obtained after annealing at 1000 °C.

excitation intensity at 980 nm and the result is also shown in Fig. 5 (triangles). It is known that the intensity of the upconverted luminescence, I_o, is proportional to some power n of the excitation intensity I_i, i.e., $I_o \propto I_i^n$, where $n = 2, 3, \ldots$. For the interpretation of the upconverted luminescence, it is often assumed that n is the order of the upconversion process, i.e., the number of pump photons required to populate the emitting state and is determined from the slope of the line of the graph of intensity versus pump power. The experimental data has been fit with a straight line with slope of ~2 (quadratic), which confirms that this emission line is a two-photon (or pair) absorption process which indicates this is a cooperative emission. Results reveal that the crystal structure, crystal size and dopant concentration are important but crystal structure and dopant concentration are more important in rare-earth doped nanocrystals. Our analysis of the dynamics of the luminescence showed that the rise time of the UPC signal peaked at 490 nm is faster for the sample with lower Yb^{3+} ions (1.25 mol%). The rise time is single exponential and the value is 1.1 ms for Yb^{3+}–Tm^{3+} (1.25:0.25 mol%) co-doped ZrO_2 nanocrystals. However, with increasing the concentration of Yb^{3+}, the bi-exponential curves are observed. The values are 1.6 and 9.5 ms for Yb^{3+}–Tm^{3+} (2.5:0.25 mol%) co-doped ZrO_2 nanocrystals and 1.5 and 8.1 ms are for Yb^{3+}–Tm^{3+} (5.0:0.25 mol%) co-doped ZrO_2 nanocrystals. The luminescence rise is related to the lifetime of intermediate excited states involved in the UPC processes. Note that the longer time constant of the bi-exponential curves is the same order of magnitude of the excited state lifetime of Yb^{3+}. This indicates that the importance of Yb^{3+} ions in the UPC process observed in our samples. There is another channel competing at higher Yb^{3+} ions doping with the population loading

of excited state of Tm^{3+}, viz., cooperative UPC as shown in Fig. 4.

4. Conclusions

In summary, we have observed infrared-to-blue upconversion in Yb^{3+}–Tm^{3+} co-doped ZrO_2 nanocrystals under near-infrared radiation (980 nm). We have shown that the crystal structure, crystal size and UPC emission can be tuned by controlling the Yb^{3+} concentration. Our results highlight the importance the role of Yb^{3+} ions on crystal structure, crystal size and upconverted luminescence property of Yb^{3+}–Tm^{3+} co-doped ZrO_2 nanocrystals. We have also confirmed that the pump power dependence of blue (490 nm) UPC emission is cubic indicating that three excitation photons are involved in the UPC process. However, the pump power dependence of the emission at 505 nm is quadratic, indicating that this emission is cooperative UPC from pairs of Yb^{3+}. In conclusion, we must say that concentration of Yb^{3+} ions has played a major role on blue upconverted emission in Yb^{3+}–Tm^{3+} co-doped ZrO_2 nanocrystals.

Acknowledgments

A. Patra and S. Saha thank Dr. H.S. Maiti, Director of CGCRI for his constant encouragement and active co-operation to carry out the work. We acknowledge the financial support by the Department of Science and Technology (NSTI, No.SR/S5/NM-05/2003). G.S. Maciel thank C.B. de Araújo for sharing equipments and he acknowledges CNPq for financial support.

References

[1] F. Auzel, Chem. Rev. (Washington, DC) 104 (2004) 139.
[2] M. Pollnau, D.R. Gamlein, S.R. Luthi, H.U. Gudel, Phys. Rev. B 61 (2000) 3337.
[3] D. Matsuura, Appl. Phys. Lett. 81 (2002) 4526.
[4] H. You, T. Hayakawa, M. Nogami, Appl. Phys. Lett. 85 (2004) 3432.
[5] E. De La Rosa-Cruz, L.A. Diaz-Torres, R.A. Rodriguez-Rojas, M.A. Meneses-Nava, O. Barbosa-Garcia, P. Salas, Appl. Phys. Lett. 83 (2003) 4903.
[6] S. Heer, O. Lehmann, M. Haase, H.U. Gudel, Angew. Chem. Int. Ed. 42 (2003) 3179.
[7] A.R.S. Niedba, H. Feindt, K. Kordos, T. Vail, J. Burton, B. Bielska, S. Li, D. Milunic, P. Bourdelle, R. Vallejo, Anal. Biochem. 293 (2001) 22.
[8] A. Patra, C.S. Friend, R. Kapoor, P.N. Prasad, J. Phys. Chem. B 106 (2002) 1909.
[9] A. Patra, C.S. Friend, R. Kapoor, P.N. Prasad, Chem. Mater. 15 (2003) 3650.
[10] A. Patra, C.S. Friend, R. Kapoor, P.N. Prasad, Appl. Phys. Lett. 83 (2003) 284.
[11] M.A.R.C. Alencar, G.S. Maciel, C.B. de Araújo, A. Patra, Appl. Phys. Lett. 84 (2004) 4753.
[12] A. Patra, Chem. Phys. Lett. 387 (2004) 35.
[13] P. Li, I-.Wei. Chen, J.E. Penner-Hahn, J. Am. Ceram. Soc. 77 (1994) 1281.
[14] D. Michel, L. Mazerolles, M.P. Jorba, J. Mater. Sci. 18 (1983) 2618.
[15] C.Y. Chen, R.R. Petrin, D. Cyeh, W.A. Sibley, Opt. Lett. 14 (1989) 432.
[16] G.S. Maciel, A. Biswas, P.N. Prasad, Opt. Commun. 178 (2000) 65.